Eur. Phys. J. D **18**, 77–81 (2002)
DOI: 10.1140/e10053-002-0009-4

THE EUROPEAN PHYSICAL JOURNAL D
EDP Sciences

Structures and stability of Al_7C and Al_7N clusters

Q. Sun[1,a], Q. Wang[1], X.G. Gong[2], V. Kumar[1,b], and Y. Kawazoe[1]

[1] Institute for Materials Research, Tohoku University, Sendai 980-77, Japan
[2] Physics Department, Fudan University, Shanghai, 200433, P.R. China

Received 28 July 2001

Abstract. We report results of the atomic and electronic structures of Al_7C cluster using *ab initio* molecular dynamics with ultrasoft pseudopotentials and generalized gradient approximation. The lowest energy structure is found to be the one in which carbon atom occupies an interstitial position in Al_7 cluster. The electronic structure shows that the recent observation [Chem. Phys. Lett. **316**, 31 (2000)] of magic behavior of Al_7C^- cluster is due to a large highest occupied and lowest unoccupied molecular orbital (HOMO-LUMO) gap which makes Al_7C^- chemically inert. These results have further led us to the finding of a new neutral magic cluster Al_7N which has the same number of valence electrons as in Al_7C^- and a large HOMO-LUMO gap of 1.99 eV. Further, calculations have been carried out on $(Al_7N)_2$ to study interaction between magic clusters.

PACS. 61.46.+w Nanoscale materials: clusters, nanoparticles, nanotubes, and nanocrystals – 36.40.Cg Electronic and magnetic properties of clusters – 73.22.-f Electronic structure of nanoscale materials: clusters, nanoparticles, nanotubes, and nanocrystals

1 Introduction

The discovery of magic numbers in alkali metal clusters [1] started a new era in cluster science. The large abundance of sodium clusters with 2, 8, 20, 40... atoms in these experiments was proposed to have the same origin as the magic numbers in nuclei. Following the analogy of the nuclear shell structure, the magic numbers in alkali metal clusters were attributed to be due to the electronic shell structure. Similar to the bulk, the valence electrons of alkali atoms could be considered to be delocalized in the volume of the cluster and move in the weak (pseudo) potential of the ion-cores which could be approximated by a spherical jellium potential. The electronic levels in this potential are quantized according to the spherical orbitals, leading to the well-known electronic shell structure. Accordingly clusters with closed electronic shells are very stable and behave as superatoms very similar to the rare gas atoms. This idea had attracted much attention as it could lead to a novel class of materials with superatoms as the building blocks. As there could be many possibilities of developing such clusters with differing properties, it is hoped to pave a way for tailor-made materials.

The interesting aspect of such superatoms is that the effective number of valence electrons of a cluster can be altered either by changing their size or composition. It is, therefore, possible not only to mimic the electronic configuration of an atom in the periodic table but also to explore new possibilities which could hither to not be permitted with atoms as the building blocks. The ability to alter the composition and size at will provides an unprecedented opportunity to design clusters as superatoms. A typical example for this is found in aluminum clusters. Bulk aluminum is a nearly free electron metal. However, Al_{13} cluster behaves like a chlorine atom with nearly the same electron affinity. It has a total of 39 valence electrons which are one short of the $2p$ shell closing. This cluster, therefore, interacts strongly with alkali atoms [2]. Also when doped with C or Si, $Al_{12}Si$ with 40 valence electrons become much more stable [3,4] than Al_{13} with a large HOMO-LUMO gap. This kind of enhanced stability has also been theoretically found for Al_{19} and Al_{23} by doping with Si recently [5].

Experimental confirmation for such doped magic clusters is very crucial for future developments. Recently Leskiw and Castleman [6] have reported a large abundance of Al_7C^- cluster and its non-reactive nature with oxygen. They proposed a structure of this cluster as an AlC^- dimer interacting with Al_6 cluster. Its stability was proposed to be due to the closed shell nature of Al_6 with 18 valence electrons and of AlC^- with 8 valence electrons. However, here we show that this is not the case and that carbon interacts with Al_7 strongly occupying the interstitial position. The electronic structure of this cluster is used to explain the magic nature of Al_7C^-. Further, considering the equivalence of C^- with N, we expected neutral Al_7N to be magic. This is indeed confirmed by the present

[a] e-mail: sunq@imr.edu
[b] *Permanent address*: Dr. Vijay Kumar Foundation, 45 Bazaar street, K.K. Nagar (west), Chennai 600078, India.

Table 1. The geometric and electronic parameters for Al_7, Al_7C and Al_7N clusters. ϵ is the binding energy (eV/atom), R_m, the mean bond length between Al atoms, E_g, the HOMO-LUMO gap (eV), and SM, the spin multiplicity.

cluster	symmetry	ϵ	HOMO	LUMO	E_g	SM	R_m
Al_7	C_{3v}	2.15	$a_1\uparrow$	$a_1\downarrow$	0.7159	2	2.7198
Al_7C	C_{2v}	2.927	$a_1\downarrow$	$a_1\uparrow$	0.3355	2	2.855
Al_7N	C_{3v}	3.30	e	a_1	1.99	1	2.872

calculations which predict Al_7N to be isostructural with Al_7C but with a higher symmetry due to its closed shell electronic configuration. Clusters of aluminum nitride are interesting because it is an important wide band gap semiconductor for optoelectronic devices and is one of the best known thermal conductors with partly ionic and partly covalent bonding [7]. We, therefore, also performed calculations on a dimer of Al_7N to study interactions between such magic clusters.

In Section 2 we present the computational details while the results and a discussion is given in Section 3. Finally our conclusion is given in Section 4.

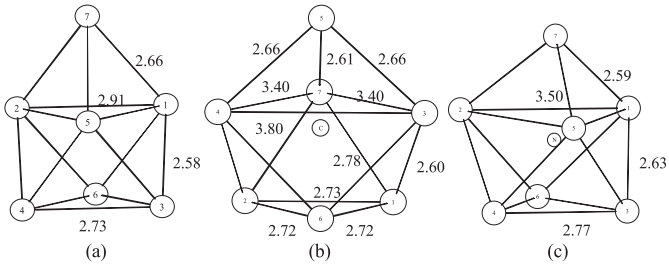

Fig. 1. Optimized structures of (a) Al_7, (b) Al_7C, and (c) Al_7N.

2 Theoretical method

We use the *ab initio* molecular dynamics method [8] based on the density functional theory (DFT) which has now become a well established tool to study structural properties of materials. In particular the plane wave basis and pseudopotential method provide a simple framework in which the calculation of Hellmann-Feynman force is greatly simplified so that extensive geometry optimization is possible. However, for carbon and nitrogen, the lack of corresponding core states for orthogonalization makes the tightly bound $2p$ valence wave functions sharply peaked. As a result, in the conventional pseudopotential scheme [8], a relatively hard pseudopotential has to be generated and a relatively large number of plane-wave basis functions are needed in the calculations. This makes the study of structural optimization of clusters containing carbon and nitrogen quite difficult. In the present calculations we use the Vienna *ab initio* simulation code [9–11] based on the ultrasoft pseudopotentials [12] and a plane-wave basis. This uses the finite-temperature density functional theory of Mermin [13] so that the variational quantity is the electronic free energy. The finite temperature leads to the broadening of the one electron levels and helps to improve the convergence of Brillouin-zone integrations.

The minimization of the free energy over the atomic and electronic degrees of freedom is performed using the conjugate gradient iterative technique [14]. We use a simple cubic supercell with 15 Å edge length for a single cluster, and 28 Å for a cluster dimer. In such a big supercell only the Γ point is used to represent the Brillouin zone. The exchange-correlation energy is calculated within the generalized gradient approximation [15] (GGA) with spin-polarization. The calculations are performed with high precision using a cut-off of 170 eV, 373 eV and 435 eV for pure Al cluster, dopping with C and N clusters, respectively. The convergence criteria for energy and force are 10^{-5} eV and 0.001 eV/Å, respectively. The structure optimization is symmetry unrestricted.

3 Results and discussions

As a test we first carried out calculations on Al_2. The ground state is found to be $^3\Pi_u$ with bond length of 2.48 Å and binding energy of 1.86 eV. These are in good agreement with the values obtained from other theoretical results [16] as well as the experimental value [17] of the binding energy (1.5 eV). In the following we discuss results on Al_7C and Al_7N clusters as well as the Al_7N dimer. The binding energies, HOMO-LUMO gaps and the mean bond lengths for Al_7, Al_7C and Al_7N clusters are given in Table 1.

3.1 Al_7C

The high stability of Al_7C^- cluster was explained in reference [6] within a jellium model. According to their interpretation AlC^-, a stable eight electron entity and Al_6 with $1d$ closed shell in jellium model combine to form Al_7C^-, *i.e.* $AlC^- + Al_6 \rightarrow Al_7C^-$. However, this explanation is not sound as we show in the following.

We consider neutral Al_7 and Al_7C clusters to understand the large abundance of Al_7C^-. The most stable structure of Al_7 is found to be a capped antiprism with C_{3v} symmetry as shown in Figure 1a. A similar result was obtained using the local spin density approximation (LSDA) by Jones [16] and the local density approximation by Kumar [18]. The bond length in the upper (lower) triangle is 2.91 Å (2.73 Å) and the nearest neighbor interatomic distance between the triangles is 2.58 Å. The bond length between the capping atom and the upper triangle is 2.66 Å. The average binding energy per atom is 2.15 eV. This is significantly lower than the LSDA value [16]. The

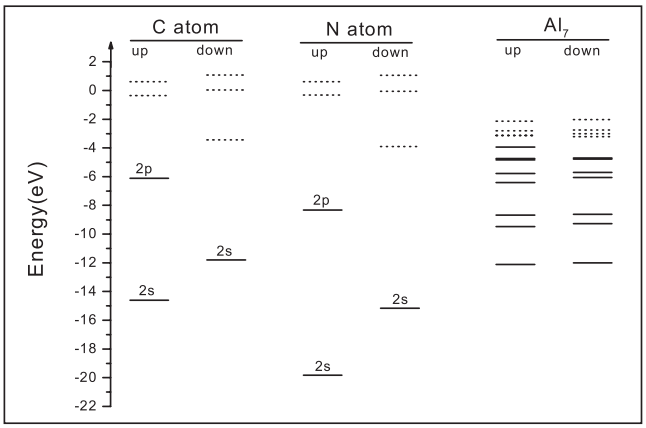

(a)

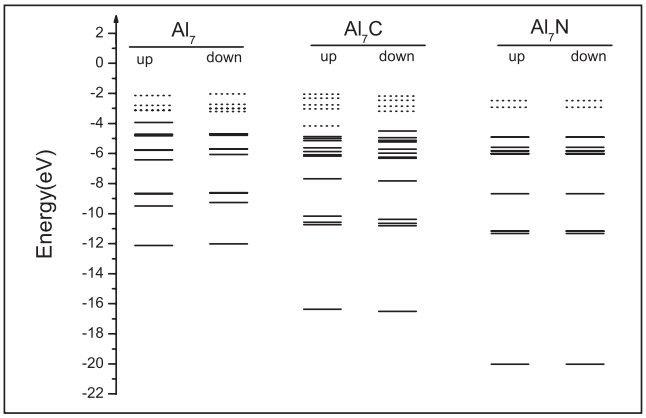

(b)

Fig. 2. Electron energy levels for (a) C atom, N atom and Al_7 and (b) Al_7C, and Al_7N clusters. The solid lines are for the occupied states and dotted lines for the unoccupied states. There is a large gap between the first and the next LUMO states of Al_7C which should make Al_7C^- magic. Also a large HOMO-LUMO gap is clearly seen for Al_7N.

energy spectrum (Fig. 2a) of Al_7 can be described within the jellium model such that $1s$, $1p$, $1d$ and $2s$ up- and down-spin states are fully occupied and the remaining electron occupies the lowest lying a_1 up-spin state derived from the $1f$ level. The LUMO is a_1 down-spin state and the HOMO-LUMO gap is 0.716 eV.

For Al_7C we tried several configurations: C on the top of the capping Al atom as well as on bridge and hollow sites with nonequivalent positions. The top site is found to be a local minimum, while for all other configurations, C atom penetrates into the Al_7 cluster to occupy the interstitial position. This is lower in energy than the top site position. The converged structure has C_{2v} symmetry as shown in Figure 1b. Note that the carbon atom is not at the center of the Al_6 antiprism but slightly displaced upwards so that the distance between the C and the capped Al atoms is 2.07 Å. This also gives rise to an increase in the interatomic distances in the upper triangle of Al_7. The binding energy increases significantly (2.927 eV/atom) due to strong interactions between the $2p$ orbitals of C with those of Al_7. As the total number of valence electrons is odd, there are slight distortions which lift the degeneracy of the states. The electronic structure of this cluster can be understood by considering interaction of a carbon atom with Al_7. From the energy spectra of Al_7 and C (Fig. 2a), it is seen that the $2s$ level of carbon lies deep in energy below the spectrum of Al_7 and even after interaction there is a deep level at around -16 eV (Fig. 2b). Therefore, this level is associated primarily with the carbon atom. The $2p$ state of carbon lies within the spectrum of Al_7 and should interact strongly. The 3 states around -10 eV are associated with Al_7–C complex and the remaining spectrum could be described such that the complex of $1d$ orbitals is partially occupied with one hole. The physical picture for Al_7C^- is one in which there is charge transfer from the $1f$ state of Al_7 to carbon and strong interactions between the $2p$ states of carbon and the $2s$ state of Al_7 making $1d$ state as the frontier orbital. Thus in the neutral Al_7C cluster there is a hole in the $1d$ state. In the spin-polarized calculation this leads to only a small HOMO-LUMO gap of 0.336 eV followed by a larger gap. For negatively charged Al_7C cluster, the additional electron occupies this hole giving rise to a large HOMO-LUMO gap and the stability of this cluster. In the following we now consider the case of Al_7N and show that this is in fact the case.

3.2 Al_7N

As discussed above, the hole in the $1d$ state of Al_7C can be occupied by the additional electron in N so that Al_7N should have a closed electronic shell configuration. The lowest energy structure of Al_7N is found to be similar to Al_7C but with a higher symmetry (C_{3v}) as shown in Figure 1c. The distance between N and the capped Al atom is 2.12 Å. The distances from N atom to the atoms in upper and down triangles are 2.08 and 2.106 Å, respectively. These are comparable to the Al-N bond length (1.89 Å) in bulk AlN as well as (1.83 Å) in Al_3N cluster with centered triangular configuration. The latter is also found to be a very stable cluster [19]. The binding energy in Al_7N increases further to 3.30 eV/atom. Strong interactions take place between the $2p$ orbitals of N with the $1p$ states of Al_7 (see Fig. 2a). The overall spectrum of Al_7N is similar to that of Al_7C but it is more compact due to higher symmetry. The $2s$ level of N lies further deeper, as shown in Figure 2b. The spin multiplicity is found to be 1 due to the closed shell electronic configuration. The HOMO is doubly degenerate e state while the LUMO is a_1 with a large HOMO-LUMO gap of 1.99 eV. This should make this cluster to be strongly stable and abundant.

The electronegativity of nitrogen is higher than that of Al atom whereas the ionization potential of Al_7 is lower than that of Al atom. Therefore, some charge transfer should be expected to N from the rest of the cluster. As the capping Al atom is less coordinated, the frontier orbital of Al_7 is more localized around it. It was shown [18] that a chlorine atom has the top site to be of lowest energy due

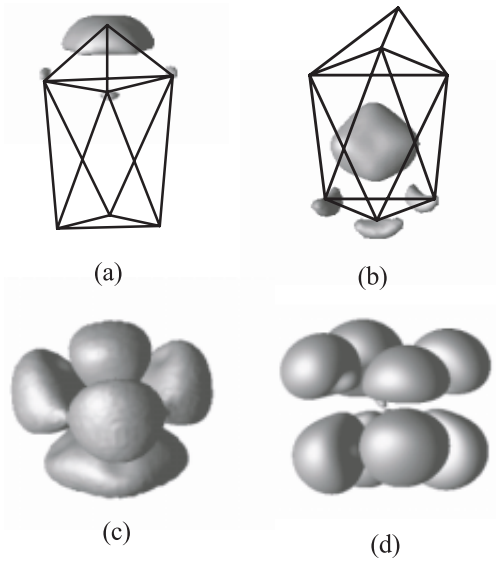

Fig. 3. Constant electronic charge density surfaces of Al_7N cluster for (a) depletion and (b) excess of charge as compared to the overlapping densities of Al_7 and N. (c) and (d) show the surfaces for the HOMO and LUMO states in Al_7N. The values of charge in the four cases are 0.036, 0.02, 0.01, and 0.006 electrons/Å^3, respectively.

to charge transfer from this state. Thus when a nitrogen atom is added to Al_7, charge transfer takes place from this capped Al atom to N atom leading to a short bond length between them. This is also borne out from the charge densities shown in Figures 3a and 3b. The constant density surfaces for the excess and depletion of charge as compared to the overlapping charge densities of Al_7 and N at the respective ionic positions in Al_7N, show that the capping as well as the three Al atoms in the upper triangle lose electrons, while N and the other three Al atoms in the lower triangle have excess of electrons. This leads to an ionic character of bonding in Al_7N cluster. The total charge densities for the HOMO and the LUMO are plotted in Figures 3c and 3d. The HOMO displays features of hybridized p and d orbitals while the LUMO exhibits the character of $1f$ orbitals. This confirms the interpretation given above for Al_7C. The overall features of the bonding appear to be similar to the one found in bulk AlN. A similar conclusion was reached by Nayak *et al.* [19] in their study of small Al_nN ($n \leq 6$) clusters.

3.3 Al_7N dimer

The HOMO-LUMO gap in Al_7N is large and similar [5] to the case of $Al_{12}Si$. It has been shown that $Al_{12}Si$ can form stable solid [20]. Therefore, it is of interest to study interactions between Al_7N clusters.

There are many possibilities for the relative orientation of two Al_7N clusters. However, from the structural features of Al_7N cluster itself, we can find the most probable orientations. Here, we consider two configurations as indicated in Figure 4. In the first one (labeled as

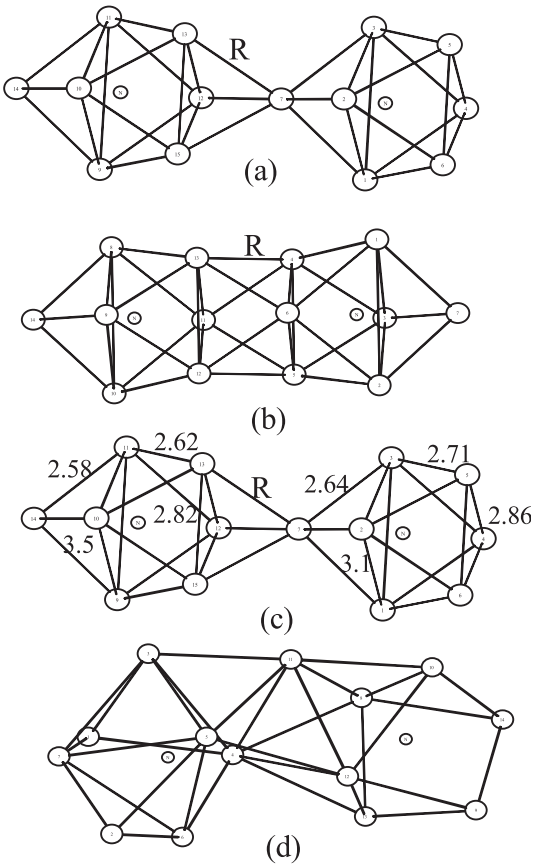

Fig. 4. Structures of Al_7N dimer with initial configurations (a) 1 and (b) 2. The corresponding optimized configurations are given in (c) and (d), respectively.

configuration 1 in Fig. 4a), the dimer is formed by bottom to top connections of the Al_7N clusters such that atom 7 becomes the common vertex for triangle capping and a centered antiprism is formed. The second one (labeled as configuration 2 in Fig. 4b) is constructed by bottom to bottom contact with a rotation of 60 degrees relative to one another. This also forms an antiprism.

In order to make the two clusters interact strongly, the initial nearest atomic distance R between the two clusters is set to be 2.5 Å, much smaller than the value in Al_7. However, after optimization, for configuration 1, R increases to 2.90 Å and the identity of the individual Al_7N cluster remains intact. The cluster still has the original symmetry, as shown in Figure 4c. This is also confirmed from the pair correlation function shown in Figure 5. It is clear that this has nearly the same features for Al_7N cluster and configuration 1 of the dimer. The total binding energy between the clusters is only 0.557 eV, while the HOMO-LUMO gap decreases to 0.745 eV. With this configuration, it could be possible to design a one dimensional cluster array like a nano quantum wire. In configuration 2 there is much stronger interaction and the net gain in energy is 1.40 eV. The nearest interatomic distance R between the two clusters is 2.68 Å which is shorter than in the case of configuration 1. Also, there is significant distortion in the original

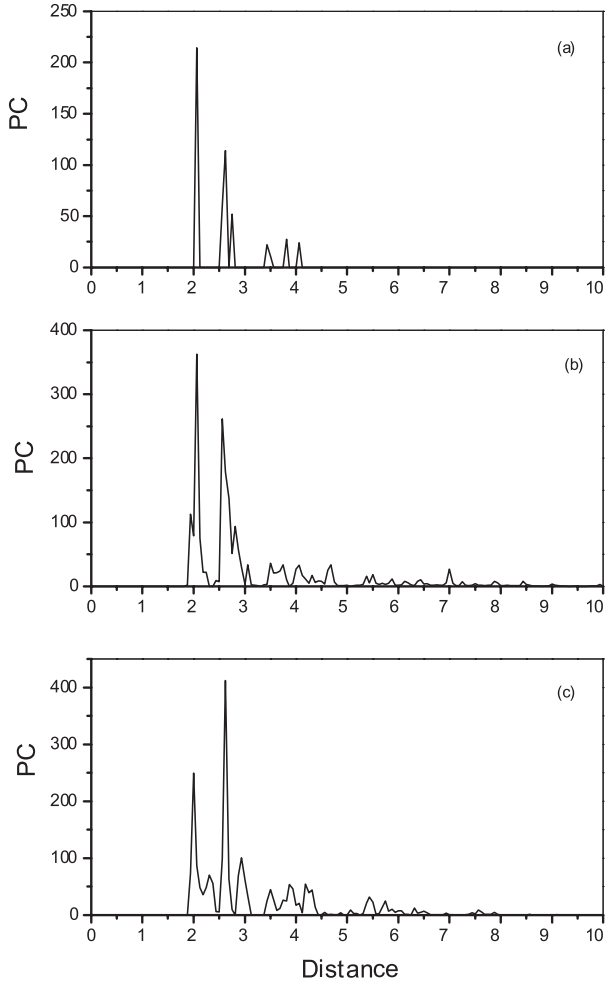

Fig. 5. Pair correlation (PC) functions (in arbitrary unit) for (a) Al_7N cluster, and optimized cluster dimer with (b) configuration 1 and (c) configuration 2. The distance is in Å.

structure of the two clusters, which is reflected in the pair correlation function in Figure 5c.

The final structure is given in Figure 4d. It appears that the non-spherical shape (low symmetry) of this cluster makes many possibilities to interact and easy to aggregate. Therefore, in order to synthesize cluster assembled materials, it seems important not only to have clusters with a large HOMO-LUMO gap but also a high symmetry of structure.

4 Summary

In summary, we have studied the atomic and electronic structures of Al_7C and Al_7N clusters using *ab initio* calculations based on the ultrasoft pseudopotential scheme and explained the stability of the observed magic behavior of Al_7C^-. The present results lead to a different structure as well as interpretation than anticipated in the experimental work. Further, we have found a new magic cluster, Al_7N, with a large HOMO-LUMO gap of 1.99 eV. However, due to the nonspherical shape, the interaction between Al_7N clusters depends on the relative orientation. It, therefore, appears that a proper control of the size, composition and shape at the atomic level could lead to a synthesis of new cluster based materials.

V.K. acknowledges the hospitality at the Institute of Materials research. The authors would like to express their sincere thanks to Materials Information Science Group of the Institute of Materials Research, Tohoku University, for their continuous support of the HITAC S-3800/380 supercomputing facility.

References

1. W.D. Knight, K. Clemenger, W.A. de Heer, W.A. Saunders, M.Y. Chou, M.L. Cohen, Phys. Rev. Lett. **52**, 2141 (1984).
2. V. Kumar, Phys. Rev. B **57**, 8827 (1998); *ibid.* **60**, 2916 (1999).
3. S.N. Khanna, P. Jena, Phys. Rev. Lett. **69**, 1664 (1992).
4. X.G. Gong, V. Kumar, Phys. Rev. Lett. **70**, 2078 (1993).
5. V. Kumar, S. Bhattacharjee, Y. Kawazoe, Phys. Rev. B **61**, 8541 (2000).
6. B.D. Leskiw, A.W. Castleman Jr, Chem. Phys. Lett. **316**, 31 (2000).
7. F.A. Ponce, D.P. Bour, Nature **386**, 351 (1997).
8. R. Car, M. Parrinello, Phys. Rev. Lett. **55**, 2471 (1985).
9. G. Kresse, J. Hafner, J. Phys.: Cond. Matt. **6**, 8245 (1994).
10. G. Kresse, J. Hafner, Phys. Rev. B **47**, 558 (1993); *ibid.* **49**, 14251 (1994).
11. G. Kresse, J. Furthmüller, Phys. Rev. B **55**, 11169 (1996).
12. D. Vanderbilt, Phys. Rev. B **32**, 8412 (1985).
13. N.D. Mermin, Phys. Rev. A **137**, 1141 (1965).
14. M.C. Payne, M.P. Teter, D.C. Allan, T.A. Arias, J.D. Joannopoulos, Rev. Mod. Phys. **64**, 1045 (1992).
15. J.P. Perdew, in *Electronic Structure of Solids*, edited by P. Ziesche, H. Eschrig (Akademic Verlag, Berlin, 1991).
16. R.O. Jones, Phys. Rev. Lett. **67**, 224 (1991).
17. C.A. Stearns, F.J. Kohl, High. Temp. Sci. **5**, 113 (1973); M.F. Cai, T.P. Djugan, V.E. Bondybey, Chem. Phys. Lett. **155**, 430 (1989).
18. V. Kumar, Bull. Mater. Sci. **20**, 745 (1997) and in *Frontiers in Materials Modelling and Design*, edited by V. Kumar, S. Sengupta, B. Raj (Springer-Verlag, Heidelberg, 1998), p. 193.
19. S.K. Nayak, S.N. Khanna, P. Jena, Phys. Rev. B **57**, 3787 (1998).
20. X.G. Gong, Phys. Rev. B **56**, 1091 (1997).